IJCRT.ORG ISSN : 2320-2882

INTERNATIONAL JOURNAL OF CREATIVE RESEARCH THOUGHTS (IJCRT)

An International Open Access, Peer-reviewed, Refereed Journal

Study Of The Flow Field Of A New Fishtail-Type Stirring Impeller In A Stirred Tank

Dr. Krovvidi Srinivas*
Department of Mechanical Engineering
Delhi Technological University
Delhi-110042
srinivaskrovvidi@dtu.ac.in

Sahil Jain[1]
Department of Mechanical Engineering
Delhi Technological University
Delhi-110042
sahiljain_2k21me235@dtu.ac.in

Rishi Kaushik[2]
Department of Mechanical Engineering
Delhi Technological University
Delhi-110042
rishikaushik_ae21b17_45@dtu.ac.in

Rishit Saini[3]
Department of Mechanical Engineering
Delhi Technological University
Delhi-110042
rishitsaini_ae21b17_46@dtu.ac.in

Prakhar Mishra[4]
Department of Mechanical Engineering
Delhi Technological University
Delhi-110042
prakharmishra_me21b17_37@dtu.ac.in

***Abstract*—The effect of design parameters on the final output of an impeller is discussed where its intrinsic design properties like blade angle, shaft length in combination to its rotational rpm were studied. These parameters were optimized using surface roughness methodology and simulated using ansys, which gave us output combination among all possible iterations.**

Keywords—Blade angle, Impeller, shaft length, simulation, CFD analysis, Optimisation

I. INTRODUCTION

Mixing is crucial in industries like pharmaceuticals, food production, and environmental engineering, ensuring uniform temperature, concentration, and phase distribution for product consistency, safety, and energy efficiency. Processes such as polymerization, solvent blending, and vaccine formulation rely on stirred tank reactors (STRs), where impellers transfer kinetic energy to induce turbulence and circulation. Mixing efficiency depends on impeller type, blade geometry, rotational speed, and vessel positioning [1]. The impeller's design is crucial, impacting power use, flow dynamics, shear distribution, mixing time, and mass transfer rates. Conventional designs— such as Rushton turbines, pitched-blade turbines, anchor mixers, helical ribbon mixers, and hydrofoils—each offer advantages but require trade-offs between efficiency, speed, and shear sensitivity [2]. To overcome these limitations, Recent fluid dynamics innovations use bio-inspired engineering, exemplified by the fishtail impeller. Modeled after sunfish caudal fins, it mimics natural propulsion to improve fluid motion while minimizing energy loss, providing a more efficient mixing solution.

II. DESIGN PARAMETERS

A. *Impeller Charecteristics*

The fishtail impeller, inspired by the caudal fin of a sunfish, features curved, tail-like blades designed for efficient mixing. This design is not just visually distinctive but purposefully optimized to generate directional flow while minimizing hydraulic resistance and energy dissipation. It enhances axial flow, reduces stagnant zones, and minimizes energy loss. The fishtail impeller functions by rotating on a vertical shaft within a cylindrical tank, its biomimetic shape generates dynamic three-dimensional flow patterns, improving overall mixing performance. [3].

The fishtail impeller's curved, bifurcated design promotes structured, symmetrical flow, improving macromixing and minimizing dead zones. Unlike flat-blade impellers, it enhances fluid movement and energy efficiency. Its blade inclination angle (θ) is crucial for regulating flow intensity, ensuring uniform mixing while reducing recirculation pockets and optimizing overall performance. A steeper angle boosts turbulent kinetic energy (TKE), accelerating turbulence and shortening mixing time. However, unlike high-shear impellers that generate concentrated shear stress, the fishtail impeller disperses energy more evenly throughout the tank, reducing mechanical stress on suspended solids and biological cells while maintaining efficient fluid motion.[4]

The fishtail impeller enhances pumping efficiency, measured by flow ($Q/N \cdot D^3$) and power (Np) numbers. Its optimized blade design increases fluid displacement while reducing energy use. With minimal input and strong circulation, it supports sustainable industrial mixing and maintains effective process control.

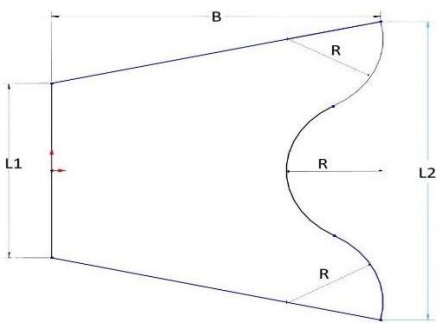

Fig no. 1 Blade Profile

B. *Design Procedure involved*

The implementation of the fishtail blade design in SolidWorks followed a structured approach to ensure precise geometric representation while maintaining accuracy and efficiency[5].

i. A new part document was created in SolidWorks, with the Front Plane designated as the primary sketch plane to define the blade profile. This setup ensured proper alignment and accuracy in modeling the fishtail blade geometry.

Base Profile Sketching:

ii. A reference coordinate system was set at the origin to ensure precise alignment of the fishtail blade geometry.

iii. A horizontal line measuring 11.7 mm (L1) was drawn from the origin, defining the base width, a vertical line measuring 20 mm (L2) was drawn perpendicular to (L1) establishing the blade height Fig no. 1.

iv. At its endpoint, a horizontal line of 17.5 mm was drawn perpendicular to (L2), defining the outer width of the fishtail blade.

Fishtail Contour Creation:

v. To achieve the characteristic fishtail shape, corner fillets were applied using the Fillet tool with a radius of 5 mm (R=5mm).

vi. The contour was then completed by connecting the remaining endpoints with lines, ensuring a fully enclosed profile while maintaining structural integrity.

Blade Inclination Implementation:

vii. To define the blade inclination, a reference plane was created at various angles relative to the Front Plane.

viii. The fishtail profile was then projected onto this reference plane using the Convert Entities tool, ensuring that the blade maintains its geometric integrity while achieving the intended inclination angle.

Disk Creation:

ix. A circle with a radius of 26.25 mm was sketched on the Front Plane, centered at the origin to ensure proper alignment.

x. The Boss-Extrude feature was then applied with a thickness of 2 mm to generate the disk, maintaining structural integrity and ensuring a stable mounting surface.

Shaft Modeling:

xi. On the same Front Plane, a circle with a radius of 5 mm was sketched concentrically with the disk to maintain alignment.

xii. The circle was extruded to the required lengths using the Boss-Extrude feature, creating a shaft that extends appropriately on both sides.

xiii. The shaft was centrally aligned with the disk to ensure balance and stability in the impeller assembly.

Pattern Generation for Multiple Blades

xiv. Circular Pattern Creation:

xv. The Circular Pattern feature was used to replicate the blade arrangement, with the central axis of the shaft defined as the pattern axis for correct rotational alignment.

xvi. The fishtail blade was selected as the pattern feature, and six instances were created to ensure uniform distribution around the disk.

xvii. The equal spacing option was enabled, maintaining a 60° separation between adjacent blades, and the pattern direction was configured for a full 360° rotation.

xviii. Final Assembly Verification:

xix. The completed impeller assembly was examined for geometric accuracy and dimensional compliance, with interference detection conducted to confirm no overlapping elements, and mass properties calculated to ensure balance and optimal structural integrity.

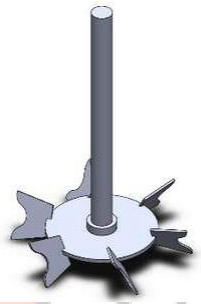

Fig no. 3 Blade and Shaft Isometric view

C. *Rationale for Design Parameters*

The specific dimensions and parameters were selected based on both theoretical considerations and empirical evidence from previous studies:[6]

- **Number of Blades (6):** A six-blade configuration provides the optimal balance between mixing efficiency and power consumption. Too many blades increase power usage without significantly improving mixing, while too few blades reduce fluid circulation, affecting performance.
- **Blade Height-to-Tank Ratio (H/10):** Positioning the impeller at a height-to-tank ratio of H/10 ensures effective fluid circulation throughout the tank. This setup prevents dead zones at the bottom while maintaining uniform mixing across the entire tank volume.
- **Blade Thickness (1mm) and Disk Thickness (2mm):** The selected dimensions balance structural integrity and material efficiency. The thicker disk (2 mm) provides a stable mounting platform, while the thinner blades (1 mm) minimize fluid resistance and reduce power consumption.

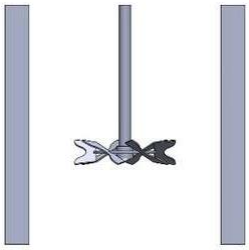

Fig no. 4 Blade and Shaft boundary enclosure

III. Simulation Boundary Conditions

A. Computational Domain and Boundary Conditions

For CFD analysis, the mixing tank was a 200 mm diameter, 200 mm height cylindrical vessel. The computational domain had two zones: a rotating zone for the impeller and a stationary zone for the rest of the tank. A sliding mesh approach ensured accurate impeller-fluid interaction modeling. Water, with standard room-temperature properties, was the working fluid for consistency [7]. The numerical framework closely matched PIV experimental results and CFD predictions for fishtail impellers, validating its reliability. The inclined fishtail blade impeller, inspired by biomimetic principles, optimized traditional geometries to enhance mixing efficiency while reducing energy consumption in stirred tanks [8].

B. CFD Simulation Using Sliding Mesh Method in ANSYS Fluent

This section outlines the simulation methodology for assessing the hydrodynamic performance of an inclined fishtail impeller in a stirred tank using the sliding mesh approach from standard CFD tutorials. This method ensures realistic transient fluid-impeller interactions. The setup includes rotating and stationary zones, with water at room temperature for consistency [8]. Validated computational frameworks provide insights into mixing efficiency, turbulence characteristics, and power consumption of the biomimetic impeller design.

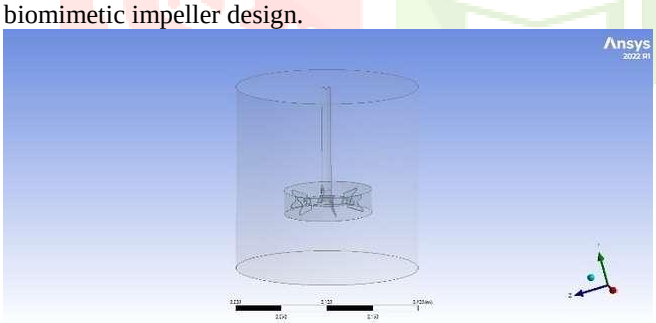

Fig no. 5 Blade and Shaft Ansys Design Modeller

C. Geometry and Domain Creation

The 3D stirred tank geometry was designed in SolidWorks and imported into ANSYS DesignModeler, featuring a 200 mm diameter and height cylindrical tank, a 6-blade fishtail impeller, and a shaft. To dynamically capture impeller rotation the domain was split into:

- A rotating cylindrical fluid zone was defined, enclosing the impeller and shaft to capture their rotational motion.
- A stationary fluid zone was established to represent the rest of the tank, ensuring interaction with the moving components.
- A cylindrical interface between the rotating and stationary zones enabled mesh motion via the sliding mesh method, ensuring accurate simulation of transient fluid behavior around the impeller.

D. Meshing

Meshing was carried out in ANSYS Mesher with specific refinements near the impeller blades, shaft, and baffles to ensure accurate flow resolution. The meshing steps followed are:

- **Unstructured tetrahedral mesh** for flexibility in handling complex geometries.
- **Inflation layers** (5 layers, growth rate ~1.2) were applied near walls and impeller surfaces to enhance boundary layer resolution.
- **Named Selections**:
  i. fluid-tank, inner-tank, impeller, shaft
  ii. outer-wall, upper-wall, bottom-wall
  iii. Interface boundaries - u1, u2
- Mesh Quality Validation:
  i. Skewness < 0.9
  ii. Orthogonal quality > 0.2
  iii. Mesh count ≈ 2.5 million elements

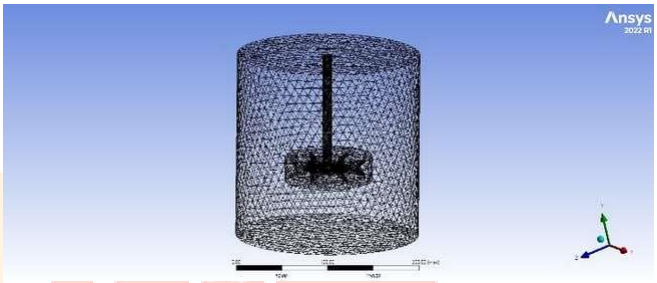

Fig no. 6 Blade and Shaft Ansys Design Mesh

E. Boundary Conditions for Simulation

The entire setup was defined in a range between the blade angle of 30^0 to 90^0, shaft length of 113 mm to 133 mm and the rotational rpm pf 180 rpm to 300 rpm. These parameter were randomized using Response surface methodology[10].

Table No. 1 Parameters for Simulation

S No.	Blade Angle (degree)	Speed (rpm)	Shaft length (mm)
1	30	240	123
2	75	210	128
3	75	210	118
4	60	240	123
5	60	180	123
6	60	240	133
7	45	270	118
8	90	240	123
9	45	210	128
10	75	270	128
11	45	270	128
12	60	300	123
13	75	270	118
14	45	210	118

15	60	240	113

For the above said combinations the design was simulated using ansys.

IV. SIMULATION RESULTS

The impeller was simulated in the said boundary conditions in the table above and the output characteristics of velocity, pressure and pressure dissipation rate were noted.

1) Output characteristics of velocity, pressure and pressure dissipation rate at inner tank

Table No. 2 Case Inner Tank

S No.	Blade Angle (degree)	Shaft length (mm)	Speed (rpm)	Velocity (m/sec)	Total Pressure	Turbulance Desipation Rate (Epsilon) (m^2/ sec^3)
1	90	123	240	0.43650236	0.21308902	0.59081158
2	75	128	210	0.73659881	711.15385	0.14825439
3	75	118	210	0.73530691	712.66936	0.14874223
4	75	128	270	0.94222018	1167.4488	0.25147769
5	75	118	270	0.94221805	1167.8508	0.25125674
6	60	123	180	0.53413708	442.77077	0.10608956
7	60	133	240	0.70495376	688.52018	0.16424174
8	60	123	240	0.70576756	691.82059	0.16233463
9	60	123	300	0.87547377	962.61764	0.26306026
10	60	113	240	0.71260505	715.3989	0.16119646
11	45	118	270	0.64603654	560.22869	0.36858083
12	45	128	210	0.61616498	541.69936	0.12741552
13	45	128	270	0.78884715	811.70203	0.20853153
14	45	118	210	0.62076269	554.56959	0.13065899
15	30	123	240	0.67822791	619.0356	0.16306649

2) Output characteristics of velocity, pressure and pressure dissipation rate at Fluid tank

Table No. 3 Case Fluid Tank

S No.	Blade Angle (degree)	Shaft length (mm)	Speed (rpm)	Velocity (m/sec)	Total Pressure(Pa)	Turbulance Desipation Rate (Epsilon) (m^2/ sec^3)
1	90	123	240	0.27660841	0.16944941	0.028695018
2	75	128	210	0.2065982	-4.9626357	10.165039
3	75	118	210	0.21044995	-1.9490159	10.270021
4	75	128	270	0.20671506	-4.9644584	10.176024
5	75	118	270	0.21052471	-1.9492357	10.278783
6	60	123	180	0.20396196	-27.699329	10.074673
7	60	133	240	0.20144976	-27.785948	9.9821751
8	60	123	240	0.20396708	-27.699488	10.074745
9	60	123	300	0.20396684	-27.699095	10.074763
10	60	113	240	0.20382213	-27.647542	9.8520151
11	45	118	270	0.52024167	-26.610425	26.992669
12	45	128	210	0.20424214	-27.519361	10.029902
13	45	128	270	0.20424248	-27.519345	10.02999
14	45	118	210	0.20210741	-27.58149	9.6801489
15	30	123	240	0.20151793	-27.383387	9.761762

3) Output characteristics of velocity, pressure and pressure dissipation rate at Case Average

Table No. 4 Case Average

S No.	Blade Angle (degree)	Shaft length (mm)	Speed (rpm)	Velocity (m/s)	Total Pressure	Turbulance Desipation Rate (Epsilon) (m^2/ sec^3)
1	90	123	240	0.28117345	0.17069534	0.044743664
2	75	128	210	0.22172423	15.475079	9.8791632
3	75	118	210	0.22542724	18.44329	9.9812003
4	75	128	270	0.22770612	28.495806	9.892781
5	75	118	270	0.23140427	31.432105	9.9926378
6	60	123	180	0.21313529	-14.628157	9.7977139
7	60	133	240	0.21543617	-7.888282	9.709451
8	60	123	240	0.21790871	-7.7089063	9.7993466
9	60	123	300	0.22262346	-0.18491122	9.8021624
10	60	113	240	0.21795498	-7.0073799	9.5828259
11	45	118	270	0.52372001	-10.383832	26.256491
12	45	128	210	0.21566347	-11.736697	9.7553372
13	45	128	270	0.22045175	-4.250348	9.7576711
14	45	118	210	0.2137143	-11.441798	9.4153966
15	30	123	240	0.21460775	-9.6335839	9.4981946

V. RESULTS ANALYSIS

To analyze the results, response surface methodology (RSM) was employed. RSM consists of mathematical and statistical techniques used to model, analyze, and optimize processes influenced by multiple variables[11]. This approach involves designing experiments to systematically vary input parameters, fitting empirical models—often second-order polynomials—to observed data, and using these models to identify optimal operating conditions[12].

1) Inner Tank Output Optimisaton

The results obtained from the inner tank region of the model when optimized at the desirability rate of 0.7526, the optimal values are blade angle = 63.4364^0, shaft length = 113mm, speed = 300rpm

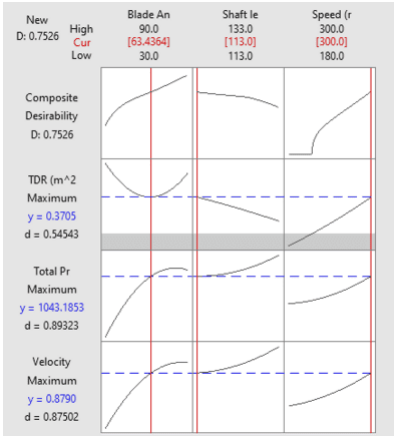

Fig no. 7 Inner Tank Optimal

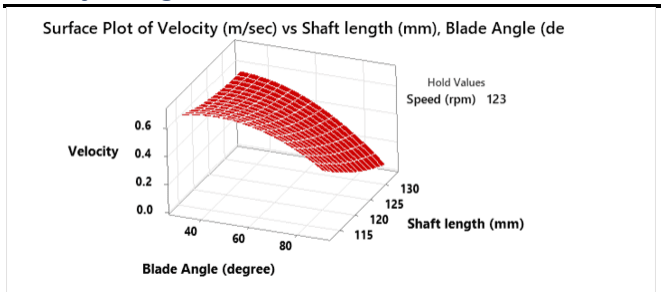

Fig no. 8 Surface Plot of Inner Tank Optimal

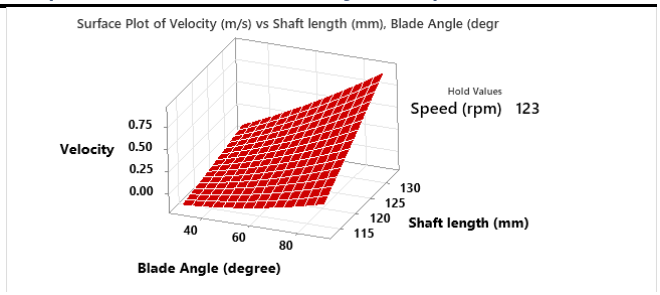

Fig no. 12 Surface Plot of case average Optimal

2) Fluid Tank Output Optimisaton

The results obtained from the fluid tank region of the model when optimized at the desirability rate of 0.7534, the optimal values are blade angle = 73.4021^0, shaft length = 113mm, speed = 180rpm.

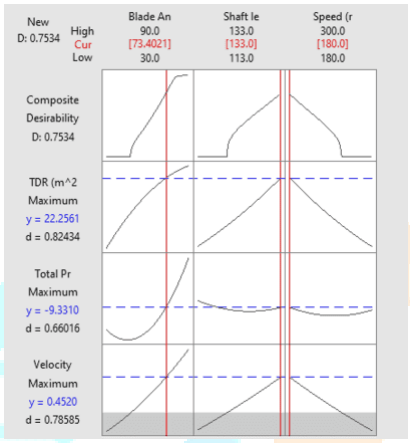

Fig no. 9 Fluid Tank Optimal

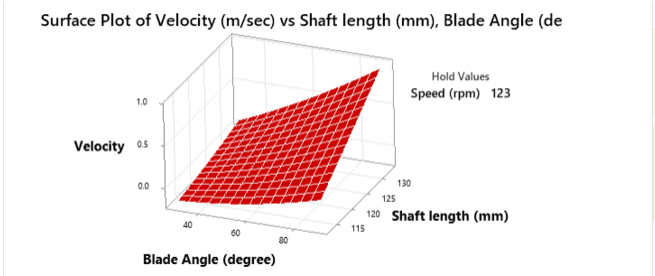

Fig no. 10 Surface Plot of Fluid Tank Optimal

3) Case average Output Optimisaton

The results obtained from the fluid tank region of the model when optimized at the desirability rate of 0.7598, the optimal values are blade angle = 90^0, shaft length = 113mm, speed = 180rpm.

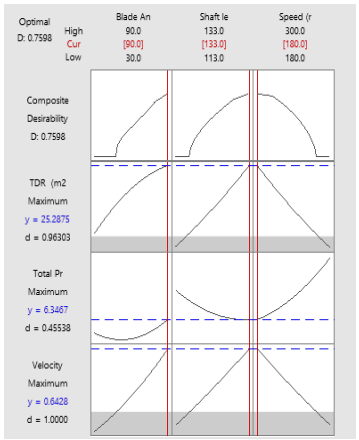

Fig no. 11 Case average Optimal

4) Mean Average of the Inner tank, Fluid tank and case average.

By considering all three output conditions the average value of the blade angle = 75.61^0, shaft length = 126.33mm, speed = 220 rpm.

When the final impeller was simulated with the above said conditions we got our final out values as follows.

Table No. 5 Optimal Simulation

	Blade Angle (degree)	Shaft length (mm)	Speed (rpm)	Velocity (m/s)	Total Pressure	Turbulance Desipation Rate (Epsilon) (m^2/ sec^3)
Case Average	75.61	126.33	220	0.22363791	17.34175	9.5943652
Case fluid Tank	75.61	126.33	220	0.20773039	-3.73166	9.8685087
Case Inner Tank	75.61	126.33	220	0.77096071	742.4051	0.16203159

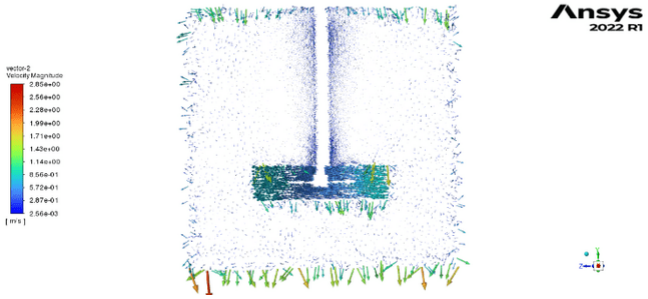

Fig no. 12 2D Vector plot of Optimal Combination

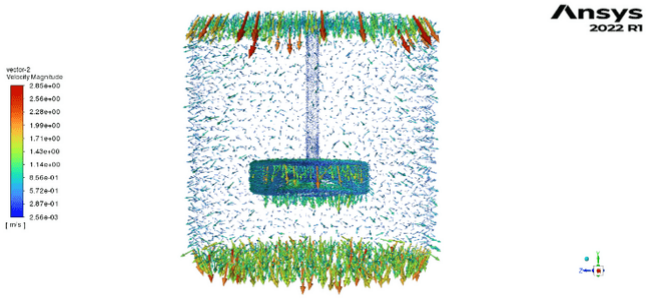

Fig no. 13 3D Vector plot of Optimal Combination

VI. Conclusion

In this work we were able to design the blade imitating a fish tail design Fig.no.1, and make act as an impeller for stirring with multiple blades and supporting shaft fig.no.3. The same setup of impeller in tank was designed in ansys fig.no.5.

This whole model was subjected different variable parameters table no.1 and simulated. Through the simulation

the values of velocity, pressure and rate of pressure dissipation were recorded. Based on these recordings the response surface methodology was implemented [13] to find out best possible combination. That resulted to be the blade angle = 75.61^0, shaft length = 126.33mm, speed = 220 rpm.

VII. REFERENCE

[1] D. Gu, H. Xu, M. Ye, and L. Wen, "Design of impeller blades for intensification on fluid mixing process in a stirred tank," *J. Taiwan Inst. Chem. Eng.*, vol. 138, no. March, p. 104475, 2022, doi: 10.1016/j.jtice.2022.104475.

[2] P. Mishra and F. Ein-Mozaffari, "Using Statistical and Experimental Methods to Investigate the Mixing of Dense Slurries with Coaxial Mixers: Effects of Design Parameters and Novel Equations for Power and Reynolds Numbers," *Ind. Eng. Chem. Res.*, vol. 60, no. 17, pp. 6306–6326, 2021, doi: 10.1021/acs.iecr.1c00090.

[3] Z. Wang *et al.*, "Study of the flow field of a new fishtail-type stirring impeller in a stirred tank," *Chem. Eng. Process. - Process Intensif.*, vol. 194, no. October, p. 109577, 2023, doi: 10.1016/j.cep.2023.109577.

[4] D. Gu, Z. Liu, F. Qiu, J. Li, C. Tao, and Y. Wang, "Design of impeller blades for efficient homogeneity of solid-liquid suspension in a stirred tank reactor," *Adv. Powder Technol.*, vol. 28, no. 10, pp. 2514–2523, 2017, doi: 10.1016/j.apt.2017.06.027.

[5] J. M. T. Vasconcelos, S. C. P. Orvalho, A. M. A. F. Rodrigues, and S. S. Alves, "Effect of blade shape on the performance of six-bladed disk turbine impellers," *Ind. Eng. Chem. Res.*, vol. 39, no. 1, pp. 203–213, 2000, doi: 10.1021/ie9904145.

[6] J. Aubin, D. F. Fletcher, and C. Xuereb, "Modeling turbulent flow in stirred tanks with CFD: The influence of the modeling approach, turbulence model and numerical scheme," *Exp. Therm. Fluid Sci.*, vol. 28, no. 5, pp. 431–445, 2004, doi: 10.1016/j.expthermflusci.2003.04.001.

[7] S. S. Deshpande, K. K. Kar, J. Walker, J. Pressler, and W. Su, "An experimental and computational investigation of vortex formation in an unbaffled stirred tank," *Chem. Eng. Sci.*, vol. 168, pp. 495–506, 2017, doi: 10.1016/j.ces.2017.04.002.

[8] I. Torotwa and C. Ji, "A study of the mixing performance of different impeller designs in stirred vessels using computational fluid dynamics," *Designs*, vol. 2, no. 1, pp. 1–16, 2018, doi: 10.3390/designs2010010.

[9] M. Ge and G. Zheng, "Fluid–Solid Mixing Transfer Mechanism and Flow Patterns of the Double-Layered Impeller Stirring Tank by the CFD-DEM Method," *Energies*, vol. 17, no. 7, 2024, doi: 10.3390/en17071513.

[10] X. Duan, X. Feng, C. Peng, C. Yang, and Z. Mao, "Numerical simulation of micro-mixing in gas–liquid and solid–liquid stirred tanks with the coupled CFD-E-model," *Chinese J. Chem. Eng.*, vol. 28, no. 9, pp. 2235–2247, 2020, doi: 10.1016/j.cjche.2020.06.016.

[11] M. Kumar, R. Gautam, and N. A. Ansari, "Optimisation of an experimental and feasibility research on a CRDI diesel engine based on a blend of waste cooking oil and waste plastic oil using RSM: A value addition for disposed waste oil," *J. Energy Inst.*, vol. 117, no. February, p. 101564, 2024, doi: 10.1016/j.joei.2024.101564.

[12] P. Kumar, M. N. Guruprasad, F. Almeida, and T. Muhammad, "Optimising the thermal characteristics of Williamson fluid flow through a microchannel influenced by the Hall effect using response surface methodology," *Case Stud. Therm. Eng.*, vol. 70, p. 106139, Jun. 2025, doi: 10.1016/j.csite.2025.106139.

[13] M. Aldandani and A. Jan, "Response surface methodology and sensitivity analysis of RP fluid model over curved stretching sheet: Non-similar investigation," *Case Stud. Therm. Eng.*, vol. 68, p. 105884, Apr. 2025, doi: 10.1016/j.csite.2025.105884.